Division of Engineering and Applied Science
California Institute of Technology
Pasadena, California

EXPERIMENTAL VERIFICATION OF CAVITY-FLOW WALL EFFECTS AND CORRECTION RULES

Contract N00014-67-A-0094-0012

by

Arthur K. Whitney
Christopher Brennen
T. Yao-tsu Wu

Report (U) No. E-97A-18

November 1970

Division of Engineering and Applied Science
California Institute of Technology
Pasadena, California

EXPERIMENTAL VERIFICATION OF CAVITY-FLOW WALL EFFECTS AND CORRECTION RULES

Contract N00014-67-A-0094-0012

by

Arthur K. Whitney
Christopher Brennen
T. Yao-tsu Wu

Report (U) No. E-97A-18 November 1970

Experimental Verification of Cavity-flow Wall Effects and Correction Rules

Abstract

This report is intended as a companion to Report No. E-111A.5, "Wall Effects in Cavity Flows", by Wu, Whitney and Lin. Some simple rules for the correction of wall effect are derived from that theoretical study. Experiments designed to complement the theory and to inspect the validity of the correction rules were then carried out in the high-speed water tunnel of the Hydrodynamics Laboratory, California Institute of Technology. The measurements on a series of fully cavitating wedges at zero angle of attack suggested that of the theoretical models that due to Riabouchinsky is superior. They also confirmed the accuracy of the correction rule derived using that model and based on a measurement of the minimum pressure along the tunnel wall.

1. Introduction

Wu, Whitney and Lin (1969) presented exact solutions for fully cavitating flows in solid wall tunnels. In particular they computed the non-lifting case of a wedge (half vertex angle, $\beta\pi$, base width, ℓ) centered in a stream limited by straight walls, h apart. Having explored the choked flow conditions in which the cavity is infinitely long and the cavitation number, σ, takes its minimum possible value, σ_c, they then treated the general case of finite cavities and came to the following basic conclusions on the influence of the wall upon the drag on the headform:

(i) The drag is always lower than that in unbounded flow at the same cavitation number, σ. The difference is termed the drag reduction. It is due to the somewhat increased velocity, decreased pressure coefficient, C_p, over the wetted surface of the body though the end points, $C_p = 1$ at stagnation, $C_p = -\sigma$ at separation are identical.

(ii) At the same σ and $\lambda = \ell/h$ the percentage drag reduction increases with decreasing wedge angle, implying that the wall effect is more significant for thinner bodies in cavity flows.

(iii) The drag reduction is almost insensitive to σ for a given wedge angle, β, and $\lambda = \ell/h$.

These effects were found with both the open-wake and Riabouchinsky theoretical models. Effects (i) and (iii) were also found for the re-entrant jet model for a flat plate $\left(\beta = \frac{1}{2}\right)$, although numerical results for other wedge angles are as yet unavailable. A review of the previous theoretical work is included in Wu, Whitney, Lin (1969) and will not be repeated here. Morgan (1966) reviews recent experimental studies of the wall effect in cavity flows. Investigations of "flow choking" and wall effect in nominally axisymmetric flow have been reported by Barr (1966), Dobay (1967) and Brennen (1969b) among others. Brennen also finds numerical solutions to the theoretical Riabouchinsky flows around a sphere and a disc and these furnish theoretical predictions of the wall effect in axisymmetric flow.

In another experimental endeavor, Meijer (1967) carried out a study of the wall effect upon a cavitating hydrofoil with flaps (nominally planar flow). He suggests an empirical method to correct for the influence of the walls. This involves the use of the minimum pressure on the tunnel wall, p_b, and the corresponding velocity, V, as reference rather than the tunnel "free stream" pressure and velocity, p_∞ and U. The usual cavitation number, σ, and drag coefficient are

$$\sigma = \frac{p_\infty - p_c}{\frac{1}{2}\rho U^2} \qquad C_D = \frac{D}{\frac{1}{2}\rho U^2 \ell S} \tag{1}$$

where p_c is the cavity pressure, D the drag on the body, ρ the density of the liquid and S the span. Meijer's corrected σ'', C_D'' are thus

$$\sigma'' = \frac{p_b - p_c}{\frac{1}{2}\rho V^2} \qquad C_D''(\sigma'') = \frac{D}{\frac{1}{2}\rho V^2 \ell S} \ . \tag{2}$$

Meijer found that this provided a satisfactory wall correction rule for his experiments. The correction rules suggested in this report are similarly based on a measurement of the minimum pressure p_b. However both the theoretical predictions of Wu, Whitney and Lin and the present experimental results indicate that Meijer's rule generally over-corrects by an amount which can be quite large.

It is of interest to point out the different trends between the wall effects in non-separated, non-cavitating flows and those in cavity flows. In closed wind-tunnels, the lateral constraint and body thickness generally result in an increase of flow velocity and hence dynamic pressure, thus increasing lift, drag, and moment coefficients at a given angle of attack (see, e.g., Pope (1954)). In contrast, the general trend of the wall effect on cavity flows in closed tunnels have been found to decrease the drag and lift coefficients at prescribed cavitation number and incidence. These opposite trends may seem at first glance puzzling, particularly to those experienced with wind-tunnel testings. Actually, the lateral constraint in the presence of a cavity still results in an increase of flow velocity and hence a decrease of the pressure over the wetted surface of the body, consequently decreasing all the forces <u>if</u> referred to the same cavitation number. Furthermore, this increase in flow velocity at the cavity boundary will cause the cavity pressure p_c

to be somewhat lower, and hence the cavitation number somewhat higher than in an unbounded flow with the same free stream condition. These two effects therefore reinforce each other such that the curve of drag coefficient, C_D, against σ lies below the corresponding curve for unbounded flow.

The first concern of the present report is the derivation of some simple rules for the correction of cavity wall effect. The second is the experimental verification of these rules and of the theoretical analyses of Wu, Whitney and Lin. However, at the same time the opportunity is taken to discuss some of the other problems and real fluid effects which arise during cavitation experiments in high speed water tunnels. These may be generally grouped as follows:

(i) Viscous effects due to the boundary layer on the model being tested.

(ii) Viscous and other effects due to the boundary layer on the tunnel walls including production of a longitudinal pressure gradient and acceleration and the possible appearance of secondary flows.

(iii) The necessity of determining the cavity pressure, p_c; effects which cause this to differ from p_V, the vapor pressure.

(iv) The determination of a hypothetical "free stream" pressure, p_∞, equal to the remote pressure were the tunnel infinitely long.

(v) Limitations on the range of cavitation number which can be satisfactorily covered including the effects of "flow choking."

(vi) Effects due to actual cavity closure. These include the unsteady, turbulent nature of the flow in this region, the cavity filling effect of the re-entrant jet (especially when this impinges on the rear of the headform) and the viscous, turbulent wake behind the cavity.

Some discussion on these is included at the appropriate point in the sections which follow.

2. Wall Correction Formulae

In view of the fact that the ratio $\lambda = \ell/h$ is usually small in experimental practice, an asymptotic representation, for λ small, of the exact solutions of Wu, Whitney, Lin (1969) can serve useful purposes for evaluating the wall effects and their corrections. The analysis of the asymptotic expansions is less complicated for symmetric wedges and will be carried out for two different flow models.

For the reader's convenience, expressions utilized in the derivations will be reproduced from Wu, Whitney, Lin (1969).

A. The Open-Wake Model

For this model, the drag coefficient is given by

$$C_D(\sigma, \lambda) = \frac{1}{\lambda U}\left(U + \frac{1}{U} - V - \frac{1}{V}\right) , \qquad (3)$$

where

$$U = (1+\sigma)^{\frac{1}{2}} \qquad (4)$$

is the upstream velocity and V is the downstream velocity. The cavity wall velocity has been normalized to unity. V depends on σ and λ through the implicit relation

$$\lambda = U[F(U) - F(V)] , \qquad (5)$$

where

$$F(U) = \frac{2}{\pi} \sin\beta\pi \int_0^1 \frac{\{1+(1-\zeta^2)^{\frac{1}{2}}\}^{2\beta} \zeta^{1-2\beta}}{\zeta^2 + [a(U)]^2} \, d\zeta \qquad (6)$$

and

$$a(U) = 2[U^{-1/2\beta} - U^{1/2\beta}]^{-1} \qquad (7)$$

In (6) and (7), $\beta\pi$ is the half-angle of the wedge.

For fixed σ (hence U), the unbounded flow limit ($\lambda = 0$) of the drag coefficient is found by letting $V \to U$ in (3) and (5), giving upon using l'Hospitol's rule

$$C_D(\sigma,0) = \frac{U^{-2}(U^{-2}-1)}{F'(U)} .$$

If this equation is solved for $F'(U)$, and integrated from U to V, an alternate expression for λ is obtained, using again (5)

$$\lambda = U \int_U^V \frac{\sigma(u)(1+\sigma(u))}{C_D(\sigma(u),0)}\, du \quad , \tag{8}$$

where $\sigma(u) \equiv u^{-2} - 1$. For a given wedge angle, (8) determines V implicitly as a function of σ and λ.

We next seek a partial differential equation for $C_D(\sigma,\lambda)$. Partial differentiation of (3) and (8) with respect to σ and λ and elimination of terms involving V gives

$$\frac{2(1+\sigma)}{\sigma} C_D(\sigma,0)\frac{\partial C_D(\sigma,\lambda)}{\partial\sigma} + \left[1 - \frac{\lambda}{\sigma} C_D(\sigma,0)\right]\frac{\partial C_D(\sigma,\lambda)}{\partial\lambda}$$

$$= \frac{1}{\lambda}\left[C_D(\sigma,0) - C_D(\sigma,\lambda)\right] + \frac{2}{\sigma} C_D(\sigma,0) C_D(\sigma,\lambda) \quad .$$

In the limit as $\lambda \to 0$, this equation becomes

$$\frac{\partial C_D(\sigma,0)}{\partial\lambda} + \frac{(1+\sigma)}{\sigma} C_D(\sigma,0)\frac{\partial C_D(\sigma,0)}{\partial\sigma} = \frac{1}{\sigma} C_D^2(\sigma,0) \quad , \tag{9}$$

or to the order of accuracy, $O(\lambda)$, we also have

$$\frac{\partial C_D(\sigma,\lambda)}{\partial\lambda} + \frac{(1+\sigma)}{\sigma} C_D(\sigma,\lambda)\frac{\partial C_D(\sigma,\lambda)}{\partial\sigma} = \frac{1}{\sigma} C_D^2(\sigma,\lambda) \quad . \tag{10}$$

For fixed σ, (10) gives an estimate of the dependence of C_D on λ, namely $\partial C_D/\partial\lambda$; however, both C_D and $\partial C_D/\partial\sigma$ must be known. For experimental applications, the latter quantity would require estimating a derivative from experimental data, which can be rather inaccurate.

A more useful result follows by integrating (10) from σ to $\sigma' < \sigma$, corresponding to $\lambda = 0(\sigma - \sigma' = O(\lambda))$, along the mathematical characteristics

$$\frac{d\sigma}{d\lambda} = \left(\frac{1+\sigma}{\sigma}\right) C_D(\sigma,\lambda) \quad , \quad \frac{dC_D}{d\sigma} = \frac{C_D(\sigma,\lambda)}{1+\sigma} \quad ,$$

and yields

$$C_D(\sigma', 0) = \left(\frac{1+\sigma'}{1+\sigma}\right) C_D(\sigma, \lambda) + O(\lambda^2) \quad , \tag{11}$$

where

$$\sigma' = \sigma - \left(\frac{1+\sigma}{\sigma}\right) C_D(\sigma, \lambda)\lambda + O(\lambda^2) \quad . \tag{12}$$

This two-way correction rule takes a measured drag coefficient $C_D(\sigma, \lambda)$, in a tunnel of known λ, and converts it by (11) and (12) to an estimated drag coefficient $C_D(\sigma', 0)$ in unbounded flow ($\lambda = 0$) at a different cavitation number, σ', given by (12). An example of the use of this rule in estimating unbounded drag coefficients from theoretically calculated data, $C_D(\sigma, \lambda)$, is shown in Fig. 1 for $\beta\pi = 15°$. The agreement of predicted estimates with calculated values of $C_D(\sigma', 0)$ is found to be excellent for all angles, with λ up to $1/6$ and σ up to 1.

Another interesting consequence of Eq. (6) is that estimates of $C_D(\sigma, \lambda)$ can be obtained if good approximations of $C_D(\sigma, 0)$ are known. For example, for wedges with $\beta\pi > 30°$ it is known that $C_D(\sigma, 0) \simeq C_o(\beta)(1+\sigma)$ is a fairly good approximation as long as $\sigma < 1$. Substituting this approximation for $C_D(\sigma, 0)$ into (8), we have

$$\lambda = \frac{U}{C_o}\left\{\frac{1}{U} + U - \frac{1}{V} - V\right\} \quad ,$$

so that

$$C_D(\sigma, \lambda) = \frac{C_o}{U^2} = C_o(1+\sigma) = C_D(\sigma, 0)$$

by (3). Thus, there is no correction for wall effect if $C_D(\sigma, 0)$ obeys the linear relation exactly and it is reasonable to expect that the correction is small if $C_D(\sigma, 0)$ follows it only approximately. This is confirmed by numerical calculations.

Another important case occurs for small angle wedges ($\beta\pi < 15°$) and σ fairly large, in which case

$$C_D(\sigma, 0) \simeq \sigma$$

is a good approximation (see Figs. 7, 8, 9, Wu, Whitney, Lin (1969)). In this case, we find

$$C_D(\sigma, \lambda) = C_D(\sigma, 0) - \frac{\lambda}{1-\lambda} \quad ,$$

which is in excellent agreement with numerical evaluations of the exact equations (3) - (7).

B. The Riabouchinsky Model

For this model, Wu, Whitney, Lin (1969) give

$$C_D(\sigma, \lambda) = (1+\sigma)\left[1 - \frac{I_-(a,b)}{I_+(a,b)}\right] \tag{13}$$

and

$$\lambda = \frac{2U}{\pi} (\sin\beta\pi)(b^2 - a^2)^{\frac{1}{2}} I_+(a,b) \quad , \tag{14}$$

where

$$I_\pm(a,b) = \int_0^1 \frac{[1 \pm (1-\zeta^2)^{\frac{1}{2}}]^{2\beta} \zeta^{1-2\beta}}{(\zeta^2+a^2)(\zeta^2+b^2)^{\frac{1}{2}}} \, d\zeta \quad . \tag{15}$$

The parameters, a and b, are related to the upstream velocity, U, and the maximum wall velocity, V, by (7) and

$$b = a(V) \quad , \tag{16}$$

respectively. In order to examine the rate-of-change of b as the 'tunnel spacing-ratio' λ is varied, and the role played by the minimum pressure p_b and the maximum velocity V on the wall, as was once investigated by Meijer (1967) (see Eq. (2)), we also introduce a new cavitation number σ'' based on p_b and V as

$$\sigma'' = (p_b - p_c)/\left(\frac{1}{2}\rho V^2\right) = V^{-2} - 1 = \sigma(V) \quad , \tag{17}$$

where $\sigma(U)$ gives the conventional cavitation number

$$\sigma = \sigma(U) = U^{-2} - 1 \quad . \tag{18}$$

The unbounded-flow limit $\lambda = 0$ is reached as $b \to a$, which implies $V \to U$ and $\sigma'' \to \sigma$. In order to estimate C_D for small λ, we expand $C_D(\sigma, \lambda)$ given by (13) in Taylor series for $|\sigma'' - \sigma| \ll 1$,

$$\frac{C_D(\sigma,\lambda)}{1+\sigma} = \frac{C_D(\sigma,0)}{1+\sigma} + (\sigma''-\sigma)\,\frac{\partial}{\partial\sigma''}\,\frac{C_D(\sigma,\lambda)}{1+\sigma}\bigg|_{b=a} + O(\sigma''-\sigma)^2 \quad . \tag{19}$$

Now, by (13), (16) and (17),

$$\frac{\partial}{\partial\sigma''}\,\frac{C_D(\sigma,\lambda)}{1+\sigma}\bigg|_{b=a} = -\left[\frac{\partial}{\partial b}\,\frac{I_-(a,b)}{I_+(a,b)}\right]\frac{db}{dV}\,\frac{dV}{d\sigma''}\bigg|_{b=a} \quad .$$

Since the functional dependence of σ'' on b is the same as that of σ on a (see (7), (16), (17), (18)), we have

$$\frac{db}{dV}\,\frac{dV}{d\sigma''}\bigg|_{b=a} = \frac{da}{dU}\,\frac{dU}{d\sigma} \quad .$$

Furthermore, from (15) it immediately follows

$$\frac{\partial}{\partial b}\, I_\pm(a,b)\bigg|_{b=a} = \frac{1}{3}\,\frac{d}{da}\, I_\pm(a,a) \quad .$$

Combining these results, we have

$$\frac{\partial}{\partial\sigma''}\,\frac{C_D(\sigma,\lambda)}{1+\sigma}\bigg|_{b=a} = -\frac{1}{3}\,\frac{d}{da}\left(\frac{I_-(a,a)}{I_+(a,a)}\right)\frac{da}{d\sigma} = \frac{1}{3}\,\frac{d}{d\sigma}\,\frac{C_D(\sigma,0)}{1+\sigma} \quad . \tag{20}$$

Upon substituting (20) in (19), the resulting equation can evidently be written as

$$\frac{C_D(\sigma,\lambda)}{1+\sigma} = \frac{C_D(\sigma',0)}{1+\sigma'} + O(\lambda^2) \quad , \tag{21}$$

where

$$\sigma' = \sigma + \frac{1}{3}(\sigma''-\sigma) = \frac{2}{3}\sigma + \frac{1}{3}\sigma'' \quad , \tag{22}$$

and σ'' is given by (17), which can either be calculated from (14) and (16) or be obtained by actual measurement in experiments. This correction rule has also been used to compare corrected estimates of $C_D(\sigma', 0)$ with the numerical results of the exact solution $C_D(\sigma, 0)$; the agreement is again excellent for wedges of all angles with $\lambda < 1/6$, $\sigma < 1$. An example is shown in Fig. 1 for $\beta\pi = 15°$. Its application in experiments will be discussed in Sect. 5.

It is noteworthy that (21) is identical to (11); only σ' is different in these two theoretically derived wall-correction rules. To this end, we note that σ' in (12) is known once σ, λ, and $C_D(\sigma, \lambda)$ are measured, whereas in (22), (17), σ'' requires an additional measurement of either V or p_b.

Another point worthy of note is that although the significance of σ'' has been explored earlier by Meijer (1967), its use in Meijer's empirical rule leads to an over-correction of the wall effect on drag coefficient. This is indicated in Fig. 1 for $\beta\pi = 15°$. This is because in Meijer's rule, σ'' takes the place of σ', instead of a weighted contribution as given by (22).

In the choked flow limit, $V \to 1$ and $\sigma'' \to 0$ and (22) becomes

$$\sigma' = \frac{2}{3}\sigma$$

so that (21) is

$$\frac{C_D(\sigma, \lambda)}{1+\sigma} = \frac{C_D\left(\frac{2}{3}\sigma, 0\right)}{1 + \frac{2}{3}\sigma} . \qquad (23)$$

This equation gives the choked flow drag coefficient if the unbounded drag coefficient as a function of σ is known, or visa versa. As an example of the use of (23) we estimate the choked flow C_D for $\beta\pi = 15°$ in Fig. 1 and compare this with the computed value.

Finally, we observe that in these two sets of wall correction rules the body configuration has become implicitly absorbed in the drag coefficient as one of its argument (i.e. $C_D(\sigma, \lambda; \beta)$). In view of the result that these correction rules are extremely accurate over the entire range of β $(0 < \beta < 1)$, it is reasonable to expect that they are also valid for bodies of arbitrary shape, at least for those with not too great curvatures of their surface profiles.

3. Experimental Arrangements

Four wedges of vertex angle $2\beta\pi = 7\frac{1}{2}°$, $9°$, $15°$ and $30°$ (chord $\approx$ 6 in.) were tested in the high speed water tunnel at the California

Institute of Technology, utilizing the 6 in. span, two dimensional working section (Kiceniuk (1964)) whose normal height is 30 inches. However by fitting the tunnel with inserts the 9° and 30° wedges were also run with a wall spacing of 13.45 in. (see Fig. 2). The models were supported in the center of the tunnel on a three component force balance for direct measurement of total drag. At the conclusion of each set of experiments the total drag forces on the fairing plate and wedge supports were measured by replacing that plate by a blank, supporting the wedge in the same position but fastened to the opposite side-wall and measuring the drag registered under conditions identical to those of the main experiments. Subtracting this tare drag from the original drag reading yielded a measure of the force on the wedge alone.

A working section reference pressure, p_T, was measured at a point in the center of the side-wall about 7 in. upstream of the leading edge of the model using a water/mercury/air manometer (see next section). The hypothetical 'free stream' velocity in the working section, U, was inferred from the difference between p_T and the pressure upstream of the convergent section. A series of static pressure taps on the lower wall (see Fig. 2) were connected to an inverted water manometer referenced to p_T for the purpose of determining the wall pressure distribution. Since some differences were observed even with no model installed in the tunnel, values more representative of the effect of the model were obtained by using these "clear tunnel" readings as datum.

All four wedges included a base pressure tapping used to measure cavity pressure, p_c, the technique employed being a familiar one (Brennen (1969a)). The pressure line is connected through a two way push pull valve to an air supply adjusted so that the air flow keeps the line free of liquid. Activating the valve cut off this supply and connected in an air/mercury/water manometer from which, following an interval of a few seconds, the difference (p_T-p_c) could be obtained.

Two of the wedges, the 9° and 30°, were built up from the basic model used by Meijer (1967) in order to utilize the static pressure tubes distributed along one face of that model. Fifteen of these were connected to a water/mercury manometer board referred to p_T in order to obtain wetted surface pressure distributions; bleeding of these lines before every reading was required to obtain reliable data.

For each model configuration data was obtained over a series of cavitation numbers, σ, at a few selected velocities, U. However, apart from the limit imposed by flow choking (i.e. $\sigma > \sigma_c$), there were certain other physical limitations upon the range of σ which could be safely and satisfactorily covered at a particular velocity. At higher velocities (35 to 50 ft/sec depending on model size) readings could be obtained only up to a certain σ, for above this either the drag exceed that measurable by the balance (120 lbs) or the vibration of the whole structure became excessive. At lower velocities (25 to 40 ft/sec depending on model size) a minimum σ was usually imposed by the fact that an excessive number of vapor/air bubbles appeared in the pressure lines when p_T was less than about 0.45 ft. of mercury. In the case of the reduced tunnel, vibration of the inserts and oscillation of the flow around them was an added hazard. In general, however, an acceptable range of σ could be obtained by combining the results at two velocities, one in the higher range, the other in the lower.

4. Experimental Results

A recurring problem in water tunnel experiments arises in determining a hypothetical, "free stream" pressure corresponding to the remote pressure, p_∞ of potential flow calculations which assume the working section to be infinitely long. In a tunnel of constant section a favorable longitudinal pressure gradient is produced by boundary layer growth on the walls. In the present tunnel this could be overcome by flairing the side walls (Kiceniuk (1964)). Then the longitudinal pressure gradient is given roughly by

$$\frac{\partial C_p}{\partial x} = \frac{2}{S}\frac{\partial S}{\partial x} - \frac{4(S+h)}{Sh}\frac{\partial \delta_D}{\partial x} \tag{24}$$

where δ_D is some mean boundary layer displacement thickness, x is the centerline distance and S(x) is the span or tunnel width. Under normal operational conditions the boundary layer is probably turbulent so that $\partial\delta_D/\partial x$ may be given by $0.038(\nu/xU)^{1/5}$

though the effective origin of x is difficult to estimate. However both the experiments of Kiceniuk (1964) and the above formula when, say, $x^{1/5}$ is of order 1 $ft^{1/5}$ and U is between 30 and 50 ft/sec indicate that $\partial C_p/\partial x$ is roughly zero when $\partial S/\partial x$ is about 0.003. Thus the flair is set at this value. Nevertheless since pressures are to be measured on the model itself it seems wise to locate the reference pressure tap as close to the model as possible, yet far enough away for the influence of the pressure field around the model to be negligible. The choice of a tap 7 in. from the leading edge of the model (see Fig. 2) involved such compromises. Theoretical estimates indicated that the pressure field influence was less than $\Delta C_p = 0.01$ at that point. Further upstream the influence of the tunnel convergent section is felt; for example 6 in. further upstream, C_p was of the order of 0.03 higher.

It will be seen that of the theoretical models that of Riabouchinsky yields results closest to the experimental measurements. To avoid confusion by profusion comparison is made in most of the figures only with that model, whilst comments on the other model will be included in the text. Typical pressure distributions on the faces of the 9° and 30° wedges are shown in Figs. 3, 4, 5 where s is measured along the wetted surface from the leading edge and $s = C$ at separation. These agree quite well with the theory though two deviations are noteworthy: (i) the lower experimental C_p close to the leading edge are probably due to a slight downward inclination of the incident stream since small negative lifts were also registered by the balance; (ii) near the trailing edge the experimental C_p are slightly above the theory, especially when the flow is close to being choked. This second effect may be partly due to the presence of small air/vapor bubbles in the tubes registering these low pressures though there may also be some contribution from the complex boundary layer flow near separation.

The coefficients of drag are plotted in Figs. 6 and 7. Graphic integration of the experimental pressure distributions yields results in excellent agreement with the Riabouchinsky model theory. The direct measurements, corrected for tare drag, showed a greater scatter and the comparison is poorer. An estimate of the skin friction component of this total drag was obtained using the Faulkner Skan solutions for the boundary layer flow near the leading edge of a wedge. Then

$$(\Delta C_D)_{\text{Viscous}} = \frac{2\sqrt{2(n+1)}}{(3n+1)} \frac{A^{\frac{3}{4}}}{\tan\beta\pi} f''(0)\left(\frac{\nu}{CU}\right)^{\frac{1}{2}} \tag{25}$$

where $n = \beta/(1-\beta)$, A represents the strength of the leading edge singularity which is estimated from the value of $(1-C_p)\left(\frac{C}{s}\right)^n$ near that point and takes a value of about unity. In the conventional notation, $f''(0)$ is a known function of β available in tables of Faulkner Skan solutions. The work of Ackerberg (1970) would indicate that the contribution of the rapidly accelerating flow near the trailing edge is small in comparison. Equation (25) yields respective values of 0.012 and 0.006 for the 9° and 30° wedge experiments and these are included in the figures, with, as can be seen, mixed results.

The more reliable data, namely the pressure integrated drag coefficients could also be compared with the results of the open-wake theoretical model. However it is clear from the agreement with the Riabouchinsky model and the difference between the two theoretical models (Wu, Whitney and Lin (1969)) that the experimental values will lie significantly below the open-wake theory except close to the choked condition where the theories virtually coincide in any case. The difference would be especially marked for small ℓ/h at moderate to high σ. Comparison could also be made with the results of the linearized theory of Cohen and Gilbert (1957). As expected the linearized theory yields values of C_D substantially greater than either the exact theory or the experiments. This is exemplified in Fig. 1 where it is seen that the linearized theoretical choked flow line is actually above the unbounded flow line for a 30° wedge. The difference is less for wedges of smaller $\beta\pi$.

Sample wall pressure distributions, referenced to clear tunnel values as mentioned in the last section, are presented in Fig. 8 for the case of the 9° wedge. Note that the cavity wake causes the experimental curves to asymptote to a non-zero C_p downstream of the cavity. Thus the actual curves correspond to a compromise on the Riabouchinsky model theory in the direction of the open-wake model (the curves for which are not shown but decrease monotonically toward a value $C_p = -\sigma$). This deviation clearly causes a slight reduction of the minimum wall pressure below the Riabouchinsky model value. This occurred consistently as can be seen from Fig. 9 where the minimum wall pressures for all model configurations are plotted against σ. Nevertheless the agreement with theory is satisfactory.

The pressure-integrated drag on the 9° and 30° wedges are corrected for wall effect using the relations (21), (22) and the experimental values of minimum wall pressure. The results are shown with the original points and the theoretical Riabouchinsky curves in Figs. 10 and 11. Clearly the results are very satisfactory since the rule collapses the points for different ℓ/h onto a single line very close to the unbounded theoretical line. The only noticeable deviation is at low σ where the experimental points lie somewhat above that theoretical curve.

5. Concluding Remarks

The two basic conclusions to be drawn from the present work are as follows:

(1) The experimental results agree very well with the theory which employs the Riabouchinsky model. Agreement with other models is less good.

(2) The rules for the correction of wall effect which are based on the Riabouchinsky model and use the value of the minimum pressure on the tunnel wall are found to be eminently satisfactory. They may indeed be applicable to a much wider variety of cavitating flow.

Acknowledgment

The authors have pleasure in expressing their appreciation and gratitude to Professor Francis Clauser for invaluable encouragement, and to the Division of Engineering and Applied Science of the California Institute of Technology for the entire support to carry out the experimental investigation using the High-Speed Water Tunnel facility of the Hydrodynamics Laboratory.

The early part of the main theoretical study was carried out under the support of the Naval Ship System Command General Hydrodynamics Research Program, SR 009 0101, and Hydrofoil Advanced Development Program S 46-06, Contract N00014-67-A-0094-0007, administered by the Naval Ship Research and Development Center, with the results reported by Wu, Whitney and Lin (1969), and the latter part, with further results presented herein, under the support of the Office of Naval Research.

References

Ackerberg, R.C. (1970) Boundary layer separation at a free streamline. Proc. of 2nd Int'l. Conf. on Numerical Methods in Fluid Mechanics, Berkeley, Calif. Sept. 15 - 19.

Barr, R.A. (1966) An investigation of the cavity flow behind drag discs and supercavitating propellers. M.S. Thesis, Univ. of Maryland.

Brennen, C. (1969a) Dynamic balances of dissolved air and heat in natural cavity flows. Jour. of Fluid Mechanics, 37, 1.

Brennen, C. (1969b) A numerical solution of axisymmetric cavity flows. Jour. of Fluid Mechanics, 37, 1.

Cohen, H. and Gilbert, R. (1957) Two-dimensional, steady, cavity flow about slender bodies in channels of finite bredth. J. Appl. Mech. 24, 170 - 176.

Dobay, G.F. (1967) Experimental investigation of wall effect on simple cavity flows. Proc. Symp. Testing Techniques in Ship Cavitation Research. Vol. 1, 175 - 230, Skipsmodelltanken, Trondheim, Norway.

Kiceniuk, T. (1964) A two-dimensional working section for the high speed water tunnel at the California Institute of Technology. ASME; Cav. Res. Fac. and Tech.

Meijer, M.C. (1967) Pressure measurement on flapped hydrofoils in cavity flows and wake flows. J. Ship. Res. 11, 170 - 189.

Morgan, W.B. (1966) The testing of hydrofoils and propellers for fully-cavitating or ventilated operation. Proc. 11th ITTC 202 - 218, Tokyo, Japan.

Pope, A. (1954) Wind tunnel testing. Second Edition. John Wiley and Sons, New York.

Whitney, A.K. (1969) A simple correction rule for wall effect in two-dimensional cavity flow. Cavitation State of Knowledge. New York: ASME.

Wu, T.Y., Whitney, A.K. and Lin, J.D. (1969) Wall effect in cavity flows. Calif. Inst. of Tech. Rep. No. E-111A.5.

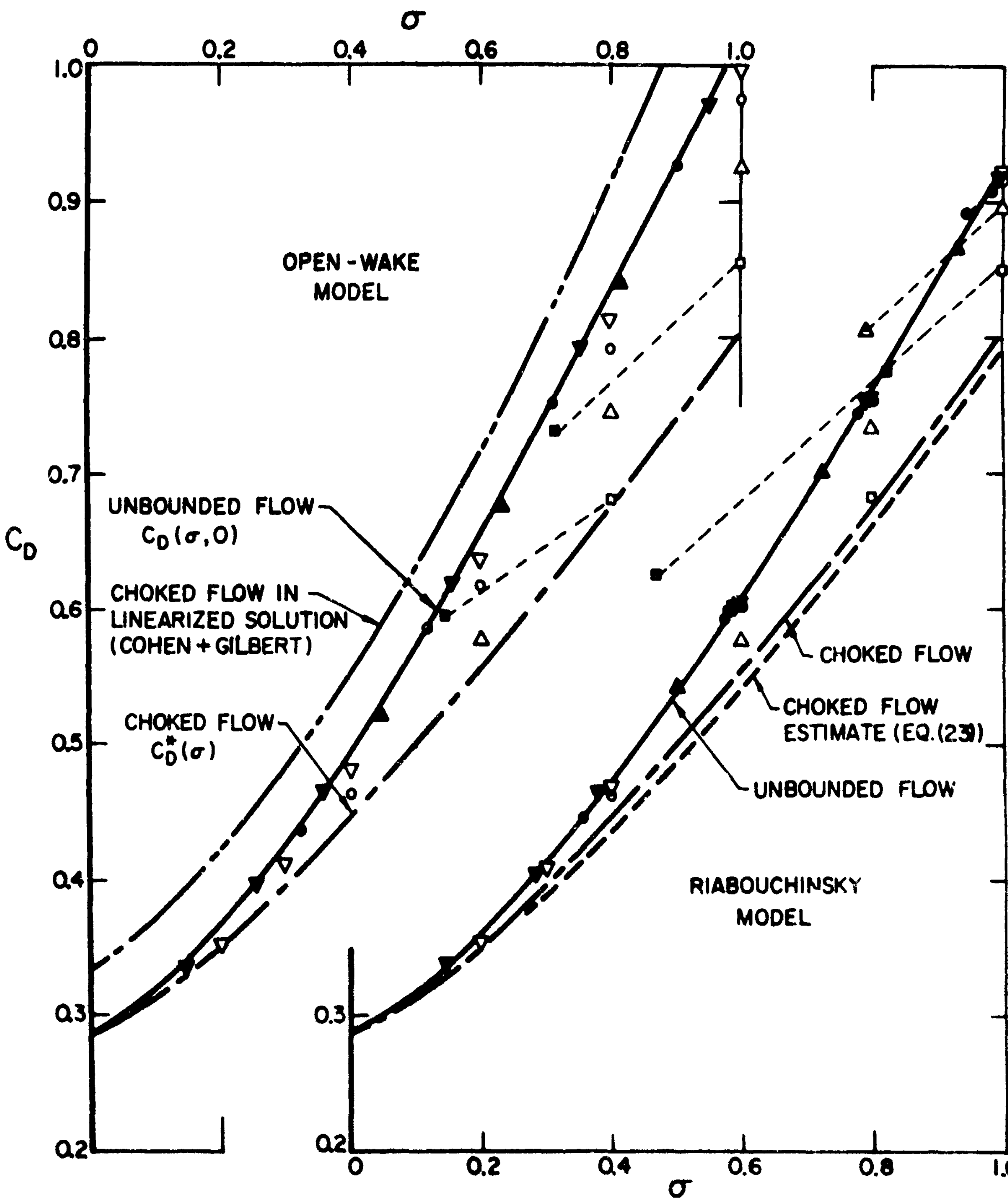

Figure 1 - Correction Rules Checked Against Theoretical Results for 30° Wedge

$\lambda = l/h$	Computed $C_D(\sigma, \lambda)$	Corrected to $C_D(\sigma, 0)$	Meijer's Corrected $C_D''(\sigma'')$
.025	▽	▼	
.050	○	●	●
.100	△	▲	▲
.167	□	■	■

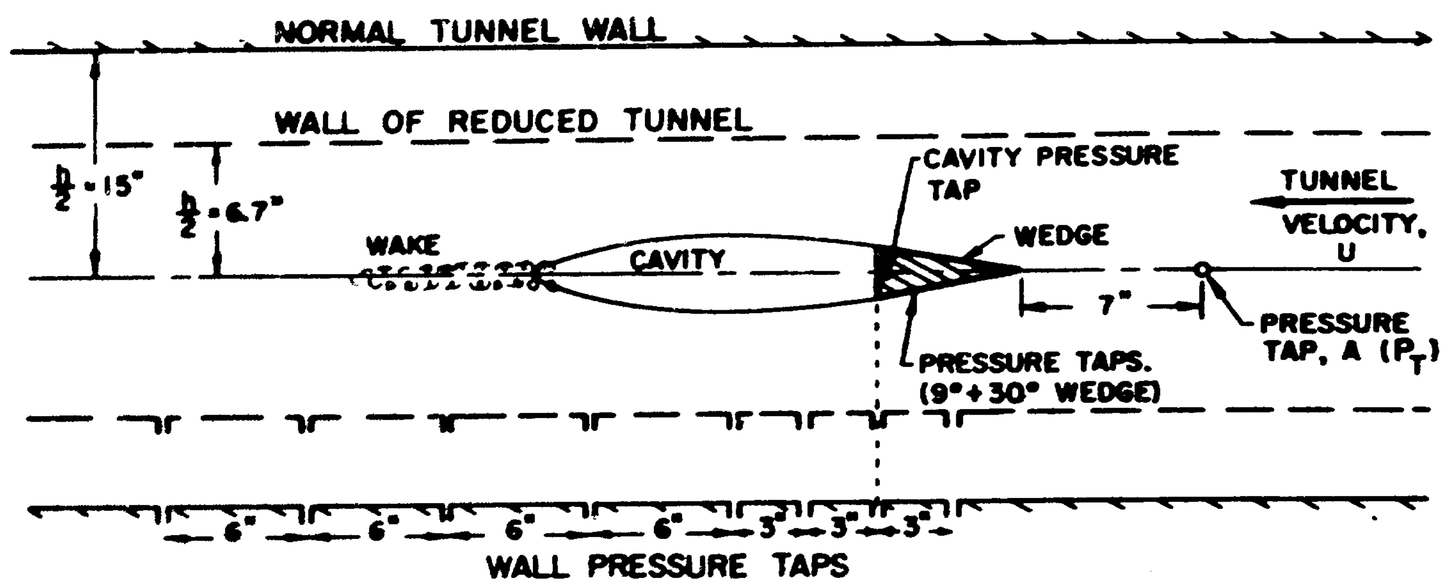

Figure 2 - Diagram of Experimental Arrangement.

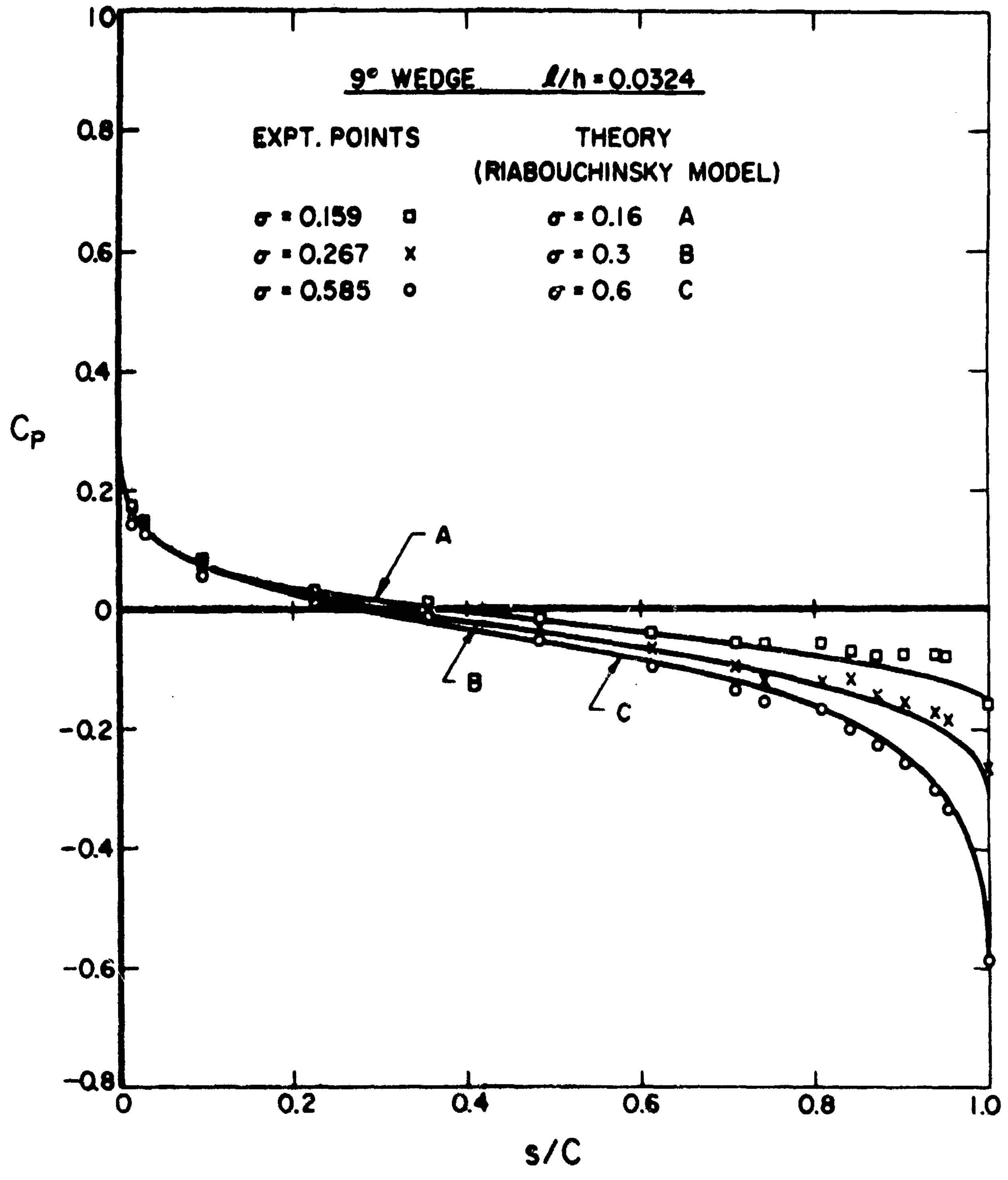

Figure 3 - Pressure Distribution on 9° Wedge in Normal Tunnel.

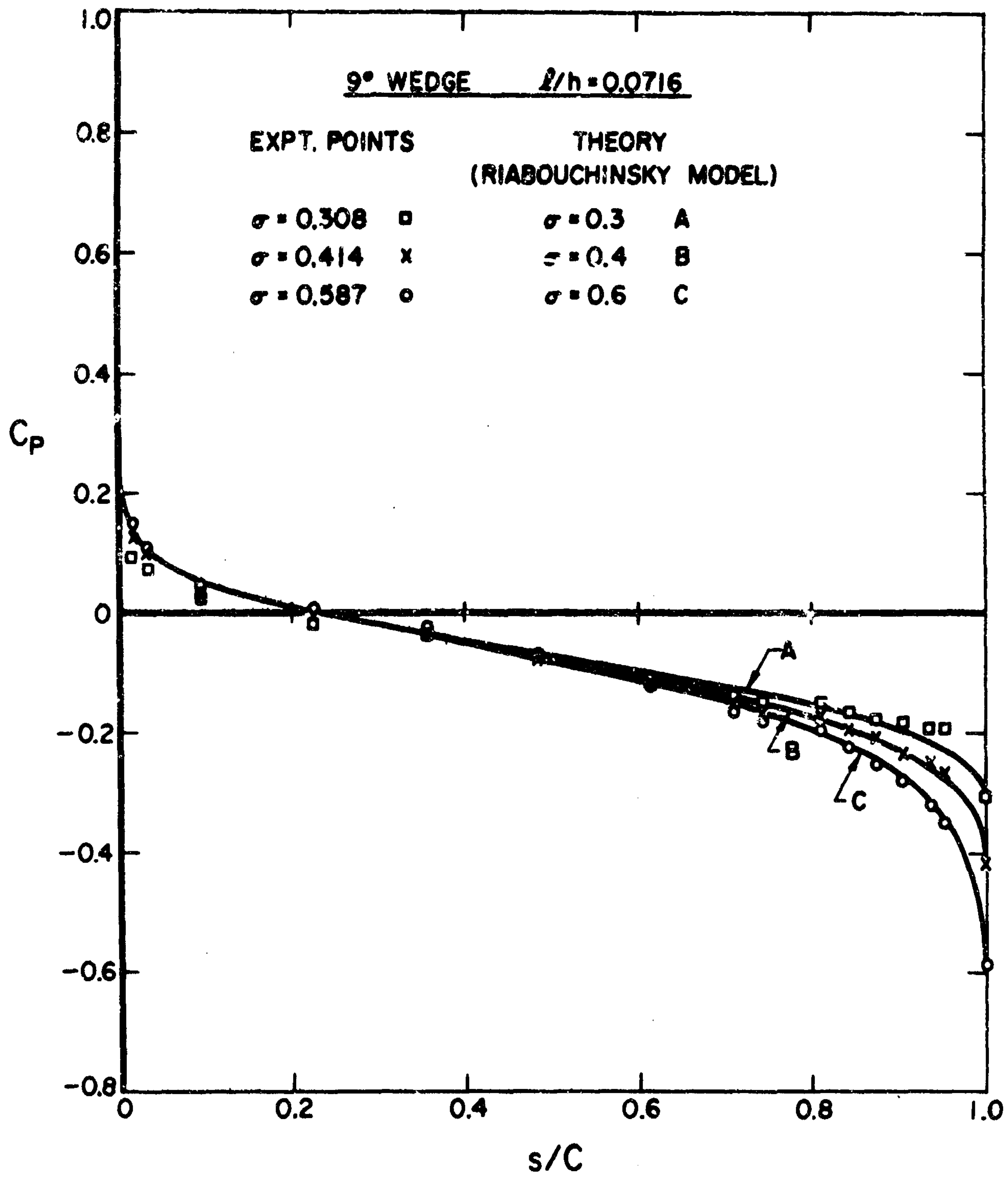

Figure 4 - Pressure Distributions on 9° Wedge in the Reduced Tunnel.

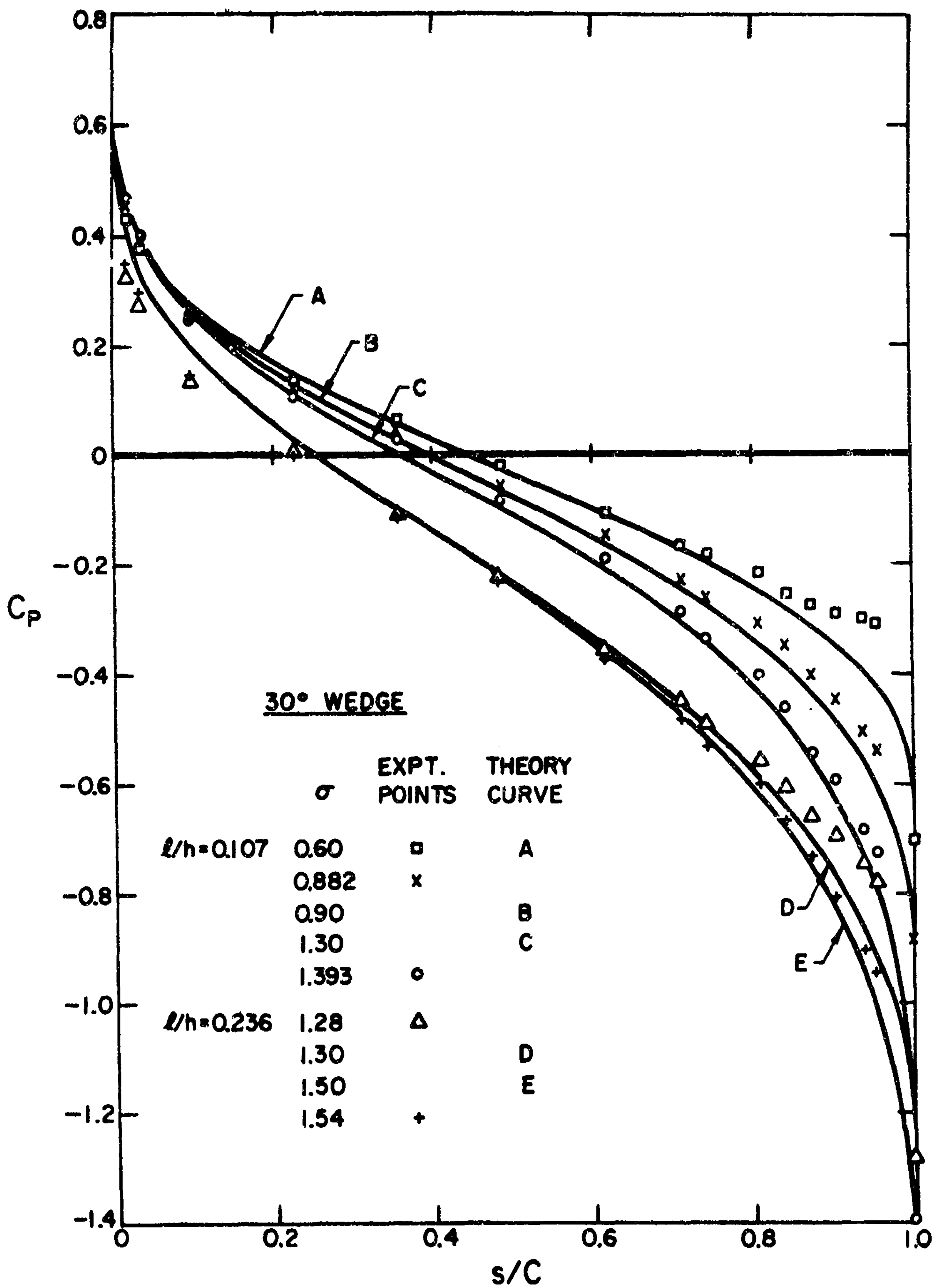

Figure 5 - Pressure Distributions on 30° Wedge.

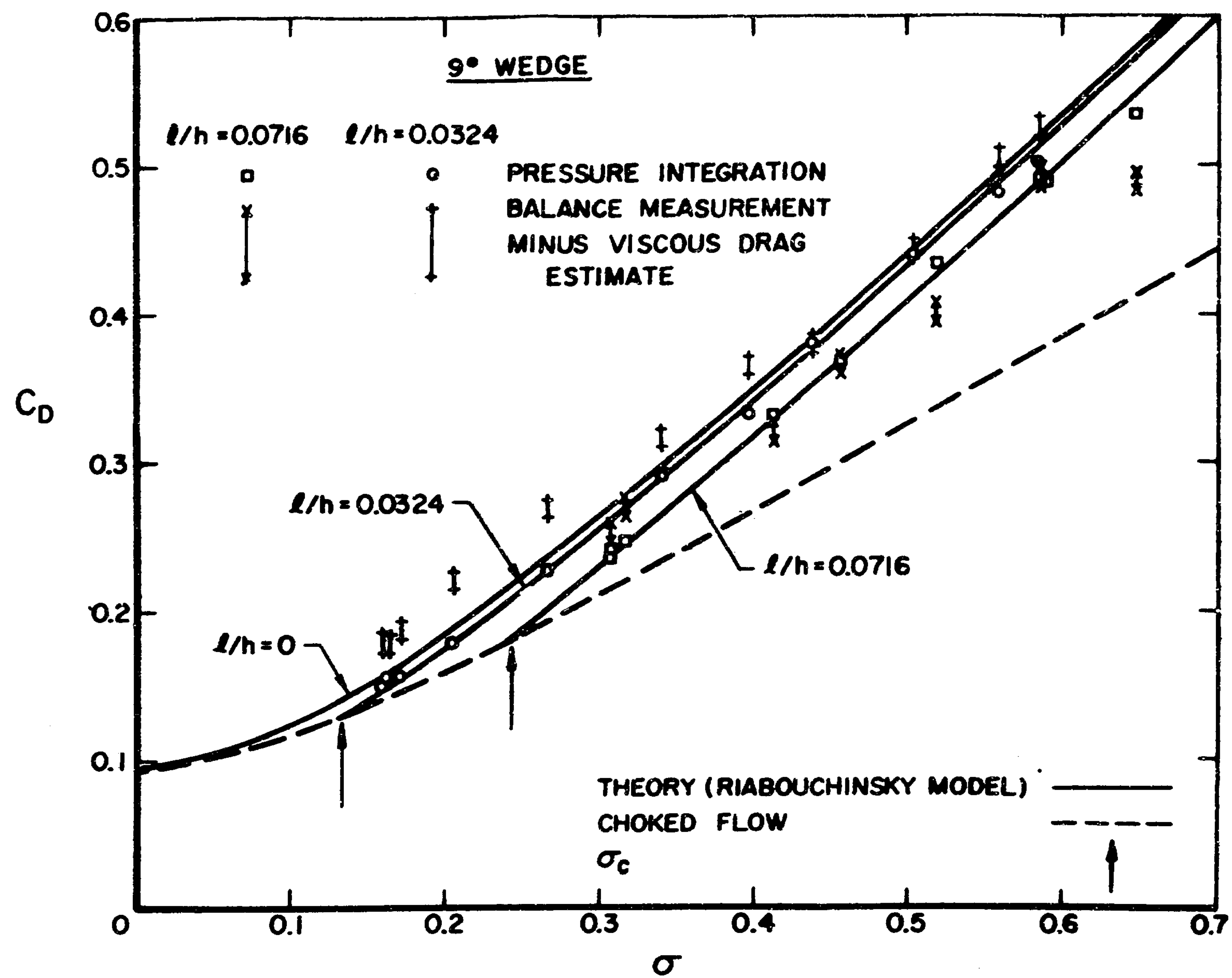

Figure 6 - Drag of 9° Wedge.

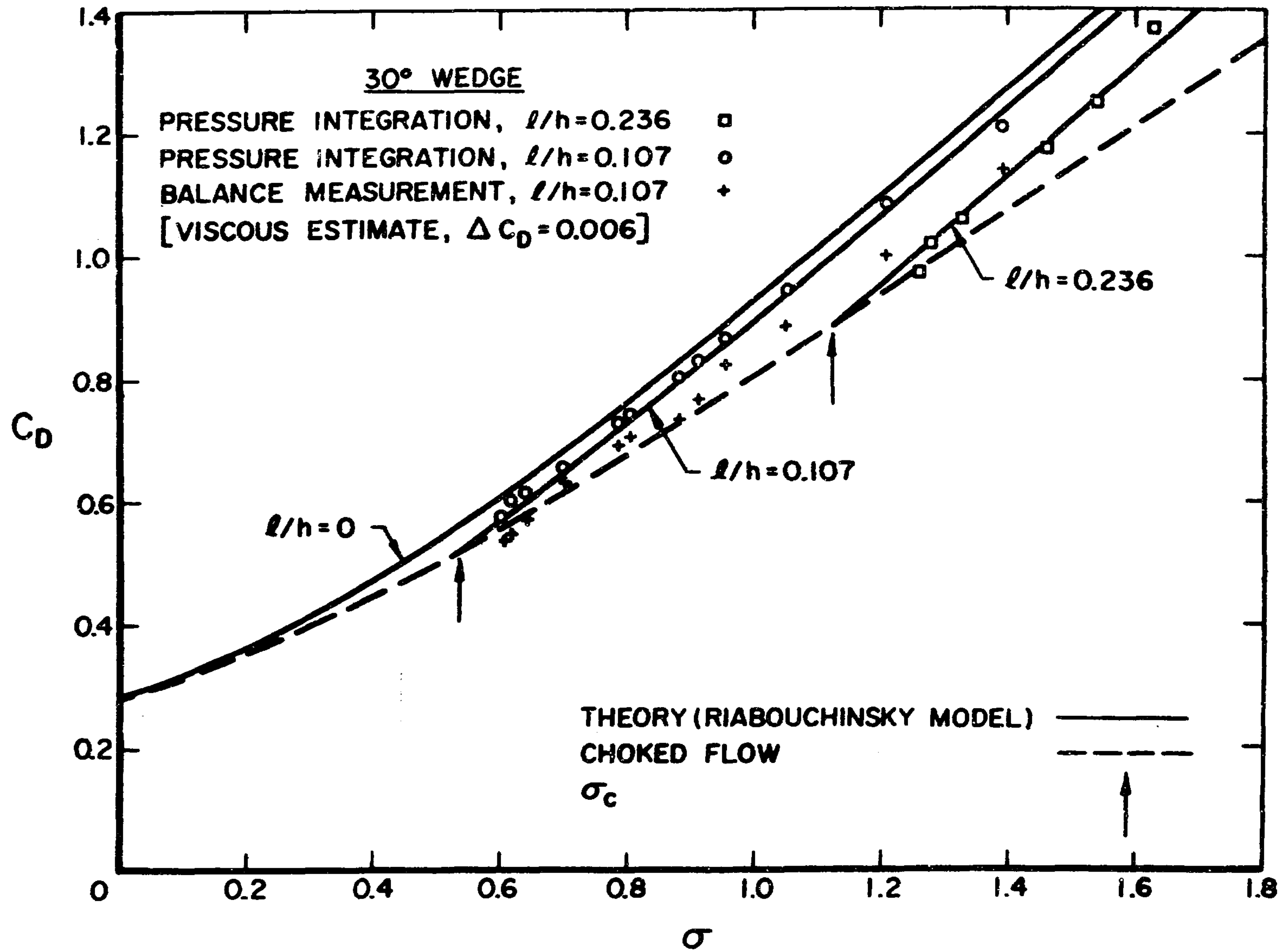

Figure 7 - Drag of 30° Wedge.

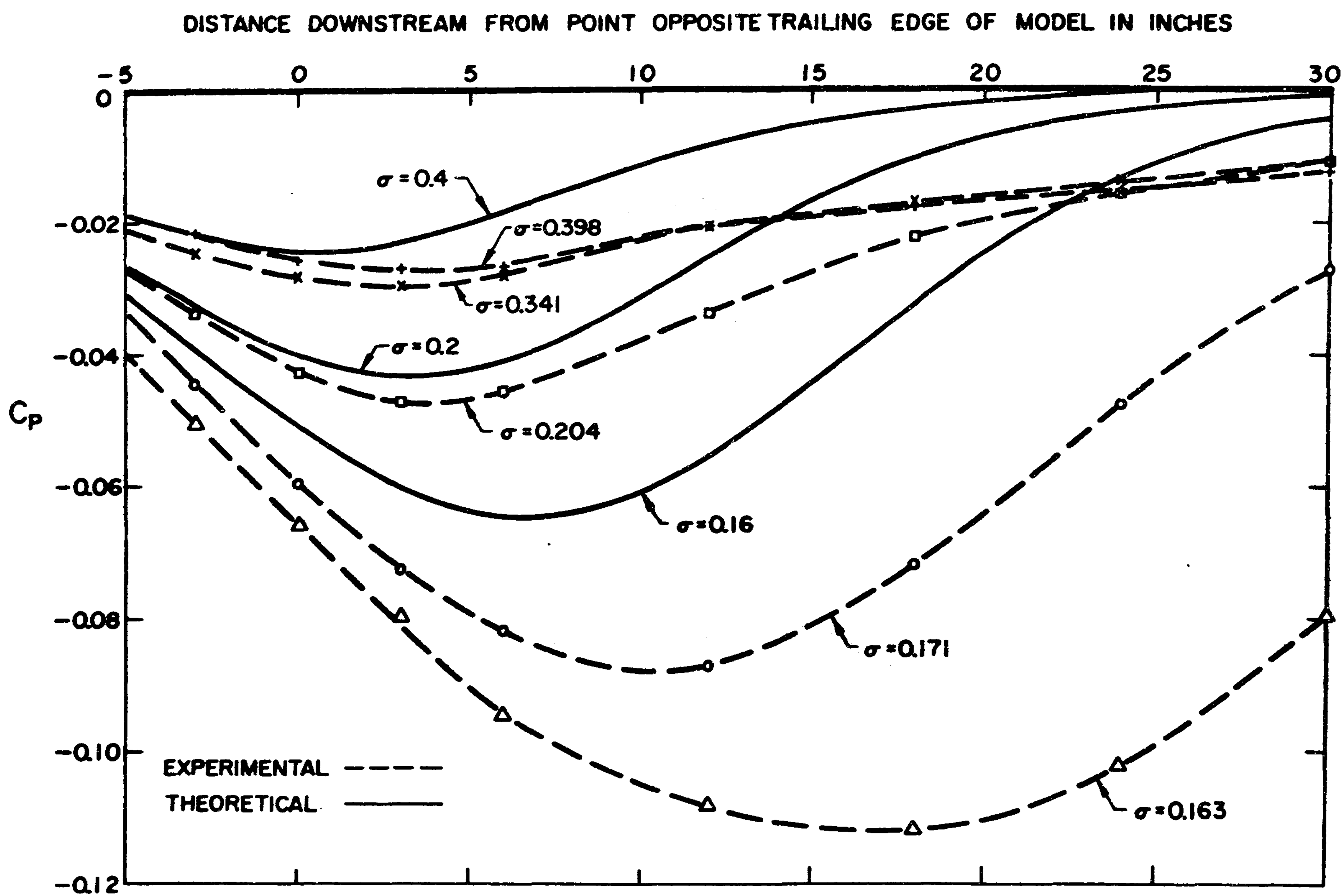

Figure 8 - Sample Wall Pressure Distributions for $2\beta = 9°$, $\ell/h = 0.0324$.

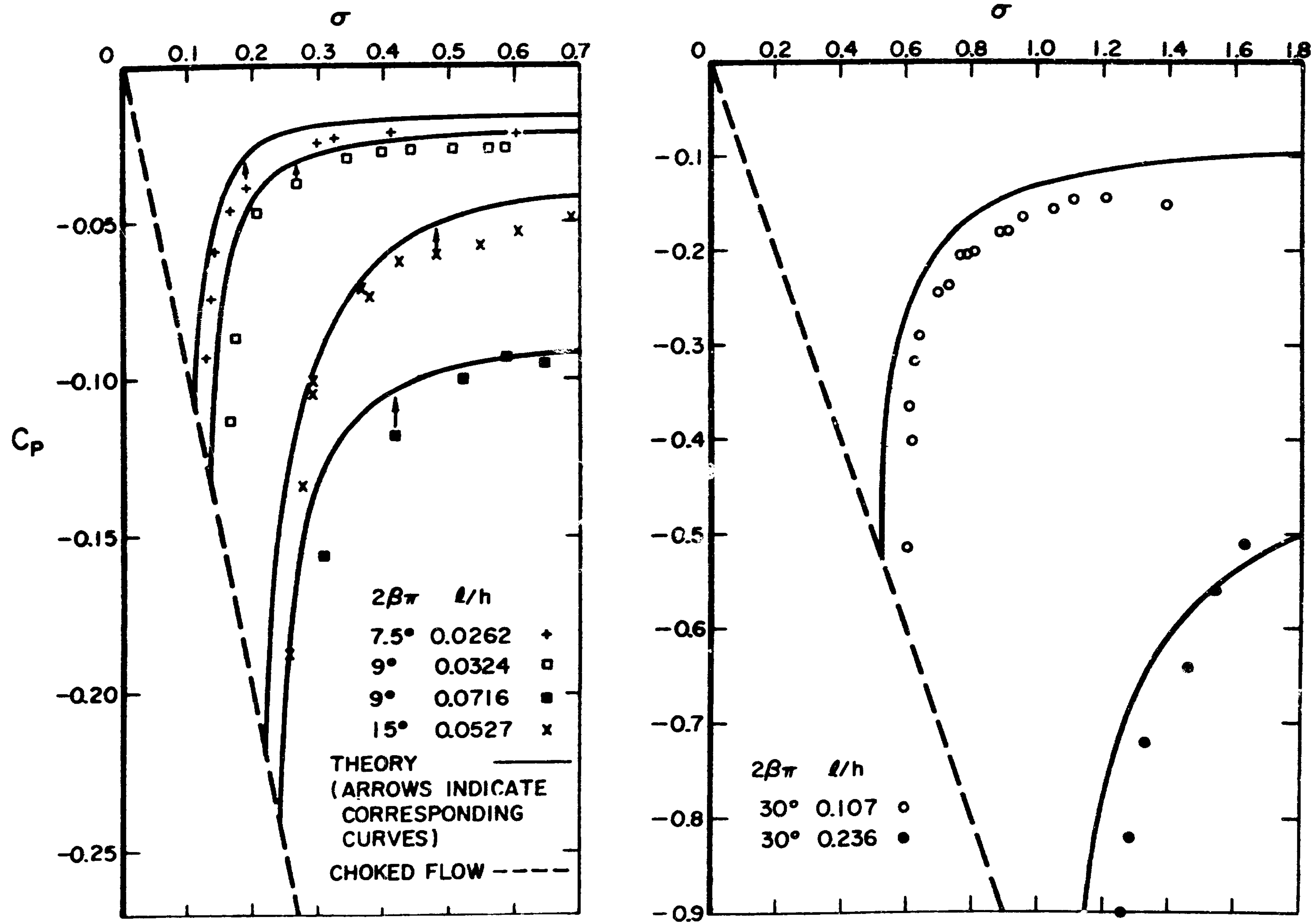

Figure 9 - Minimum Wall Pressure Versus Cavitation Number.

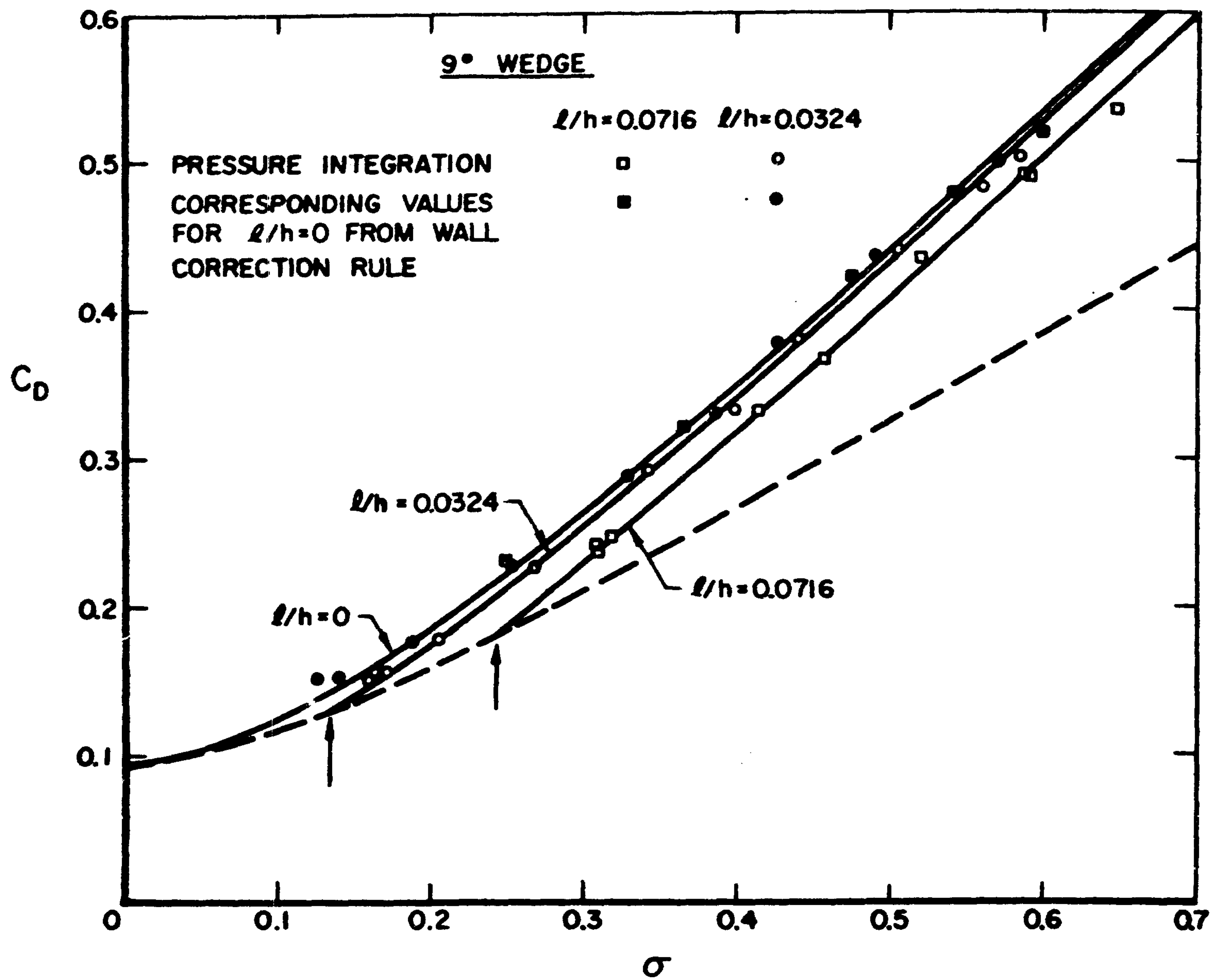

Figure 10 - Application of Wall Correction for 9° Wedge.

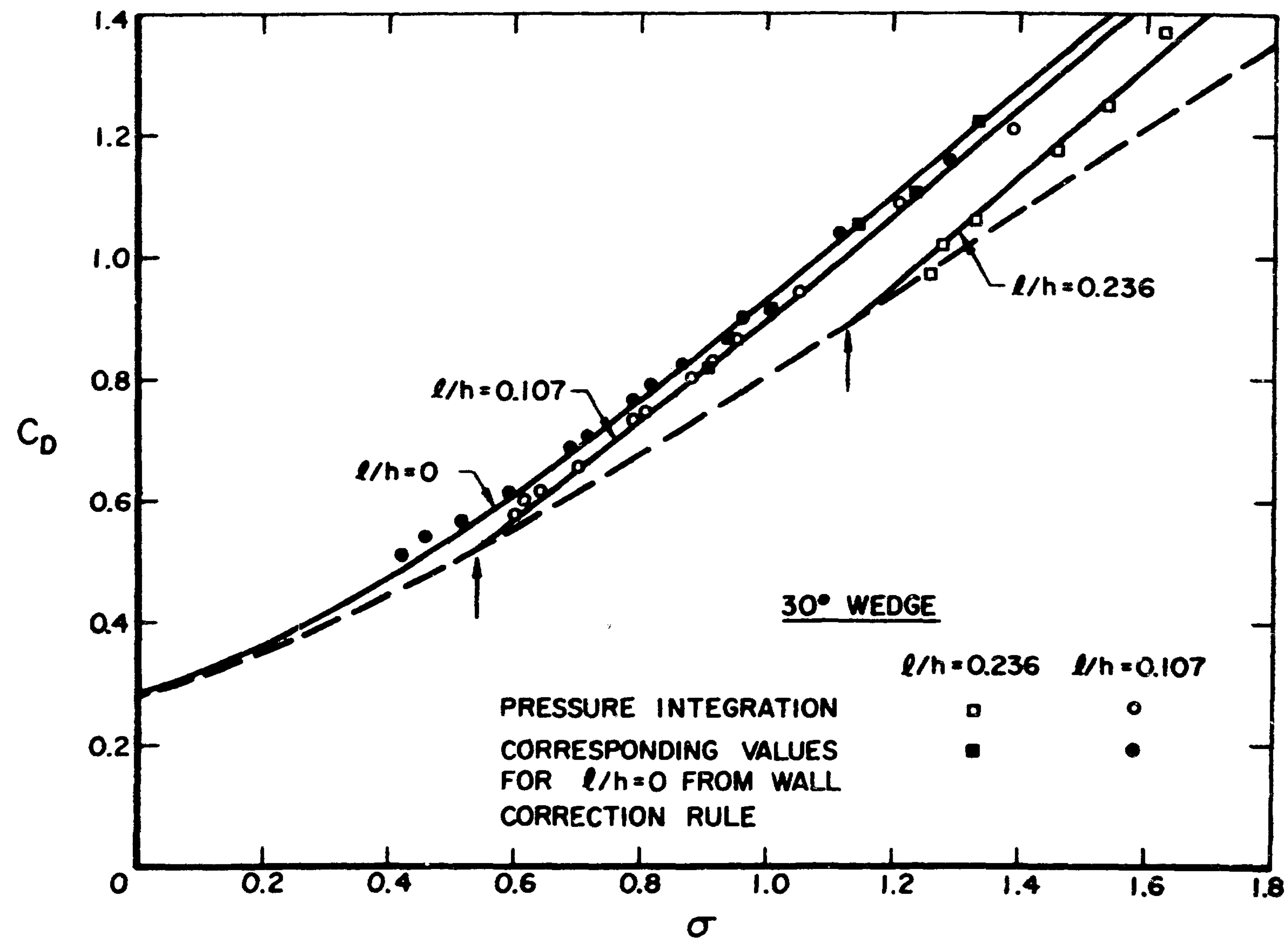

Figure 11 - Application of Wall Correction for 30° Wedge.

Unclassified
Security Classification

DOCUMENT CONTROL DATA - R & D

(Security classification of title, body of abstract and indexing annotation must be entered when the overall report is classified)

1. ORIGINATING ACTIVITY (Corporate author)
California Institute of Technology
Division of Engineering and Applied Science

2a. REPORT SECURITY CLASSIFICATION
Unclassified

2b. GROUP
Not applicable

3. REPORT TITLE
Experimental Verification of Cavity-Flow Wall Effects and Correction Rules

4. DESCRIPTIVE NOTES (Type of report and inclusive dates)
Technical Report

5. AUTHOR(S) (First name, middle initial, last name)
Whitney, Arthur K.
Brennen, Christopher
Wu, T. Yao-tsu

6. REPORT DATE	7a. TOTAL NO. OF PAGES	7b. NO. OF REFS
November 1970	28	12

8a. CONTRACT OR GRANT NO.
N00014-67-A-0094-0012

b. PROJECT NO.

c.

d.

9a. ORIGINATOR'S REPORT NUMBER(S)
E-97A-18

9b. OTHER REPORT NO(S) (Any other numbers that may be assigned this report)

10. DISTRIBUTION STATEMENT
This document has been approved for public release and sale; its distribution is unlimited.

11. SUPPLEMENTARY NOTES

12. SPONSORING MILITARY ACTIVITY
Office of Naval Research
Arlington, Va. 22217

13. ABSTRACT

This report is intended as a companion to Report No. E-111A.5, "Wall Effects in Cavity Flows", by Wu, Whitney and Lin. Some simple rules for the correction of wall effect are derived from that theoretical study. Experiments designed to complement the theory and to inspect the validity of the correction rules were then carried out in the high-speed water tunnel of the Hydrodynamics Laboratory, California Institute of Technology. The measurements on a series of fully cavitating wedges at zero angle of attack suggested that of the theoretical models that due to Riabouchinsky is superior. They also confirmed the accuracy of the correction rule derived using that model and based on a measurement of the minimum pressure along the tunnel wall.

DD FORM 1 NOV 65 1473 (PAGE 1)

S/N 0101-807-6801

Unclassified
Security Classification

Unclassified
Security Classification

14. KEY WORDS	LINK A		LINK B		LINK C	
	ROLE	WT	ROLE	WT	ROLE	WT
Cavity flow Wall effect Wall effect correction Water tunnel experiments						

DD FORM 1 NOV 65 1473 (BACK)
(PAGE 2)

Unclassified
Security Classification